

## (Dis)continuous shear thickening in frictionless granular media?

Hao Shi<sup>1,\*</sup>, Beybin Ilhan<sup>2,\*\*</sup>, Michael H.G. Duits<sup>2,\*\*\*</sup>, and Stefan Luding<sup>1,\*\*\*\*</sup>

<sup>1</sup>Multi-Scale Mechanics, Dept. Thermal and Fluids Engineering, Engineering Technology, University of Twente, Netherlands

<sup>2</sup>Physics of Complex Fluids, Science and Technology, MESA+, University of Twente, Enschede, Netherlands

**Abstract.** Continuous and discontinuous shear thickening are commonly observed in sheared dense suspensions but are still not fully understood. Although micro-friction at particle-particle contacts is widely accepted as the dominating origin of discontinuous shear thickening, if there is no interstitial fluid. With the help of discrete element simulations, we re-visit shear thinning/thickening of dry granular packings and their possible origins at the (micro) contact- and (meso) structure-scales.

The focus is here on the steady-state shear resistance of non-cohesive frictionless polydisperse sphere packings from volume fractions below random loose packing, up to higher volume fractions, above random close packing. This intermediate (transitional) regime is challenging due to its densities above the range where standard kinetic theory works, well below the statically jammed systems, only partly touching the range of dense rheology. In the frictionless packings studied here, mostly continuous shear thickening behaviour is observed, with apparent discontinuous shear thickening due to inhomogeneous shear strain.

### 1 Introduction

Granular materials are made up of many particles, as can be found in many everyday products, industrial processes and nature. Examples of granular materials include sand, soil, and many types of powders and granular substances used in the food, pharmaceutical, agriculture, and mining industries. Granular materials become even more interesting when they meet other materials, such as gases (in fluidized beds or pneumatic conveying) or fluids (in suspensions or porous media). However, there are still many open questions about their underlying micro-mechanics, physics, and potential applications

Interesting granular phenomena involve un-jamming or elasto-plastic yielding, with a variable jamming density [1], (shear) jamming [2], and (shear) dilatancy [3]. They have attracted significant interest over the past decades [4] and, remarkably, mostly can be found in frictionless particle systems. Dense suspensions of solid granules/particles immersed in a Newtonian fluid display complex flow behaviours: shear thinning or shear thickening, where the flow resistance increases when the suspension is agitated/sheared [5], in which the discontinuous shear thickening (DST) phenomenon is one of the most intriguing behaviours [6, 7].

In DST, the shear viscosity goes up dramatically (orders of magnitude) at a certain shear rate [8, 9]. Such a drastic change of flow property even allows a person to run in a swimming pool filled with a sufficiently dense cornstarch suspension – but sink when standing still [10–12].

In the present work, we shed light on the microscopic origin of continuous/discontinuous shear thickening in frictionless dense granular packings. Unlike previous studies [13–15], we neglect hydrodynamic forces in our model and only consider inter-particle contact forces. The studied volume fractions range from well below Random Loose Packing (RLP) to above Random Close Packing (RCP).

### 2 Simulation Setups

The Discrete Element Method (DEM) is a numerical method for simulating the motion of large numbers of particles, with given micro-mechanical properties, interacting through contact forces. The interactions between particles are the input needed to solve Newton's second law of motion. As the realistic modelling of contact deformations of the particles is extremely complicated, the grains are typically assumed to be non-deformable spheres, allowed to overlap.

The data directly obtained from the simulations are discrete, i.e., microscopic, and correspond to particles and contacts: they involve positions, velocities, forces, etc. To understand the constitutive behavior, the macroscopic continuum fields thus need to be extracted from the discrete data. There are in general two ways to extract continuum quantities for flow description such as density, strain, or stress from discrete particle data. The traditional one is ensemble averaging of homogeneous small samples from "microscopic" simulations, i.e., over a set of independent Representative Volume Elements (RVEs). A more recently established alternative is to simulate an inhomogeneous geometry where dynamic, dilute, flowing zones coexist

\*e-mail: h.shi-1@utwente.nl

\*\*e-mail: beybinilhan@gmail.com

\*\*\*e-mail: m.h.g.duits@utwente.nl

\*\*\*\*e-mail: s.luding@utwente.nl

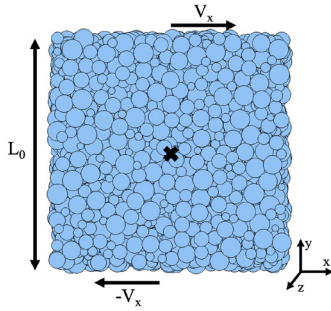


**Figure 1.** Simulation of polydisperse particles in a 3D simple shear system, using Lees-Edwards periodic boundary conditions, with displacement velocity  $V_x$  controlled to keep a constant velocity gradient (shear rate)  $\dot{\gamma} = \partial V_x / \partial y = 2V_x / L_0$ . The cross indicates the center (of mass) of the system  $(x_0, y_0, z_0)$ .

with static, higher density zones, e.g., a shear band. By using adequate local averaging over a small enough equivalent volume (inside which all particles can be assumed to behave similarly), continuum fields in a certain parameter/state window can be obtained from a single set-up [16]. In this study MercuryDPM.org, an open-source implementation of the Discrete Particle Method (DPM), is used to simulate granular flow in a simple RVE: the periodic simple shear box, see Fig. 1.

For our simple shear simulations, the initial box side lengths are set to  $L_x = L_y = L_z = L_0 = 16d_p$ , which defines the reference volume fraction  $\phi_0 = NV_p / L_0^3$ , with particle volume  $V_p = (\pi/6)d_p^3$ ; other densities are set by varying  $L_0$  accordingly. The system contains  $N = 4096$  particles of mean diameter  $d_p$ , density  $\rho_p$ , i.e., mean mass  $m_p = \rho_p V_p$ . To avoid crystallization in monodisperse systems, we use uniformly polydisperse particles, with  $w = 1.4$ , where  $w$  is the ratio of the maximum to the minimum particle size. The linear spring-dashpot normal force between particles in contact is computed as  $f_n = k_n \delta + \gamma_n \dot{\delta}$ , with overlap  $\delta$  [17, 18].

Damping,  $\gamma_n = \sqrt{[2m_s k_n (\log e_n)^2] / [\pi^2 + (\log e_n)^2]}$ , is related to the (chosen) normal coefficient of restitution,  $e_n$ , with the smallest particles' mass  $m_s = m_p / [(1+w)/2]^3$ , and the normal spring stiffness  $k_n$ , see Table 1, and the contact duration is  $t_c = \pi / \sqrt{(2k_n)/m_s - (\gamma_n/m_s)^2}$  [17].

**Table 1.** Dimensional (primed) and non-dimensional input parameters,  $Q = Q' / q_u'$ , for the contact model, as introduced in Ref. [17], with units of length  $x_u' = d_p' / 2 = 10^{-3}$  m, mass  $m_u' = 10^{-9}$  kg, and time  $t_u' = 10^{-6}$  s.

Parameter	Symbol	Dimensional SI values	Scaled values used in DEM
Average Diameter	$d_p'$	0.002 m	2
Polydispersity	$w$	1.4	1.4
Particle Density	$\rho_p'$	2000 kg/m <sup>3</sup>	2000
Normal stiffness	$k_n'$	$1 \times 10^8$ kg/s <sup>2</sup>	$1 \times 10^5$
Sliding friction	$\mu_s$	0	0
Restitution coefficient	$e_n$	0.804	0.804
Normal damping	$\gamma_n'$	2.159 kg/s	2159
Contact duration	$t_c'$	$0.49 \times 10^{-6}$ s	0.49

## 2.1 Parameters scans

To investigate continuous (or discontinuous) shear response in frictionless granular media, we systematically vary volume fraction  $\phi$  from 0.55 to 0.65 and shear rate  $\dot{\gamma}$  from  $5 \times 10^{-6}$  to 10, as summarized in Table 2.

**Table 2.** Studied volume fractions  $\phi$  and shear rates  $\dot{\gamma}$ .

	Values
$\phi$	0.55, 0.58, 0.59, 0.62, 0.63, 0.64, 0.65
$\dot{\gamma}$	$5 \times 10^{-6}$ , $1 \times 10^{-5}$ , $5 \times 10^{-5}$ , $1 \times 10^{-4}$ , $5 \times 10^{-4}$ , $1 \times 10^{-3}$ , $5 \times 10^{-3}$ , $1 \times 10^{-2}$ , $5 \times 10^{-2}$ , 0.1, 0.5, 1, 10

## 2.2 Time scales and dimensionless numbers

The flow behavior (rheology) of granular materials depends on various timescales of global and local micromechanical phenomena and interactions [19]. Each time scale can be obtained by scaling the associated parameter with a combination of different properties of material / particles, such as diameter  $d_p$ , density  $\rho_p$ , and stiffness  $k_n$ .

There are four time scales involved: the local elastic contact time scale related to the contact duration of particles determined by the contact stiffness  $k_n$ :  $t_k = \pi \sqrt{m_p / 2k_n}$ ; the microscopic relaxation time scale associated with the motion of a particle submitted to a pressure  $p$ :  $t_p = d_p \sqrt{\rho_p / p}$ ; the macroscopic time scale associated with the shear rate:  $t_\gamma = 1 / \dot{\gamma}$ ; and last but not least, the granular temperature timescale:  $t_T = d_p / \sqrt{T_g}$ , associated with the local velocity fluctuations relative to the mean flow velocity  $\bar{v}$ , defined by the granular temperature  $T_g \propto \sum_i (v_i - \bar{v})^2$ .

In general, we expect the four time scales ( $t_k$ ,  $t_p$ ,  $t_\gamma$  and  $t_T$ ) to determine the rheology. Using the ratios of these time scales, one can construct dimensionless numbers that quantify flow behavior [19, 20]. These dimensionless numbers can also be interpreted as the ratio of different forces, which signifies the relative importance of one mechanism over another. Note that among the four-time scales discussed here, there are six possible dimensionless ratios of pairs, and many other possible combinations; see Ref. [15] and the references therein. We choose three of them to define the rheology that describes our results.

The first dimensionless state variable is Softness (pressure), which happens to be the squared ratio of contact and pressure timescales:

$$p^* = p d_p / k_n = [t_k / t_p]^2 \quad (1)$$

The second is the Inertial Number

$$I = \dot{\gamma} d_p / \sqrt{p / \rho_p} = [t_p / t_\gamma] \quad (2)$$

the ratio between pressure and shear rate timescales. The last one, characterizing the fluctuation dynamics in the system, is the dimensionless Granular Temperature:

$$T_g^* = T_g \rho_p d_p / k_n = [t_k / t_T]^2 \quad (3)$$

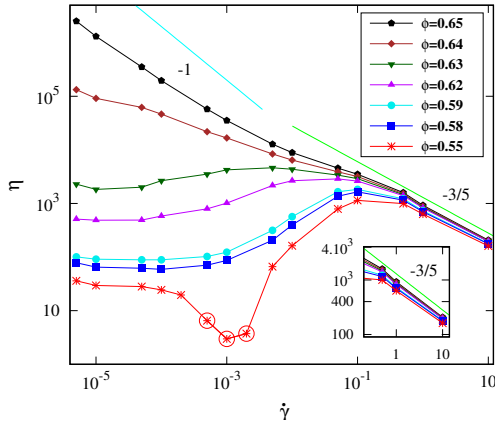


**Figure 2.** Apparent viscosity,  $\eta = \tau/\dot{\gamma}$ , plotted against shear rate,  $\dot{\gamma}$ , for different volume fractions, as given in the legend. The material is frictionless,  $\mu_s = \mu_r = 0$ , lines are guides to the eyes, and circles indicate inhomogeneous systems with layered structures.

the squared ratio between contact and temperature timescales. Other dimensionless groups were recently reviewed by Pouliquen [15], but are not discussed here for the sake of brevity.

### 3 Results at transient volume fractions

To investigate the shear behaviour of frictionless granular materials, both volume fraction and shear rate are varied, and the viscosity is displayed in Fig. 2.

For high volume fractions ( $\phi = 0.64$  &  $0.65$ ), the viscosity,  $\eta$ , decreases with shear rate, indicating a shear thinning behaviour. For intermediate volume fractions ( $\phi = 0.63$  down to  $0.58$ ), a plateau for the smallest shear rates is followed by weak continuous shear thickening (CST) at increasing shear rate.

For the largest shear rates ( $\dot{\gamma} > 0.1$ ), the viscosity data approach each other and almost collapse (see zoom inset). For the lowest volume fraction,  $\phi = 0.55$ , a kink is observed at  $\dot{\gamma} \approx 10^{-3}$ , with the viscosity dropping around one order of magnitude and increasing rapidly before joining the shear thinning behaviour for  $\dot{\gamma} \geq 0.1$ .

This kink in viscosity appears discontinuous, but it is caused by structural patterning during steady state shearing, where the particles are aligned in the shear ( $x$ ) direction, i.e., particles form separate layers along the height ( $y$ ) direction; albeit there is space between layers, particles hardly travel across layers. This effect is shown in Fig. 3, where all the particles are randomly distributed at the beginning of shearing (transient) but almost perfectly layered at the end of shearing (steady state) along the height ( $y$ ) direction. Even with layers, there is no shear band observed. Structuring can lead to a prominent increase in free space and reduction of stress or pressure and velocity fluctuations, and thus a reduced (bulk) shear resistance.

In Fig. 4, the (macro) bulk friction is plotted against  $I$ , where the dashed lines indicate the dense rheology by Shi et al. [19] that only agree for high volume fractions, at low

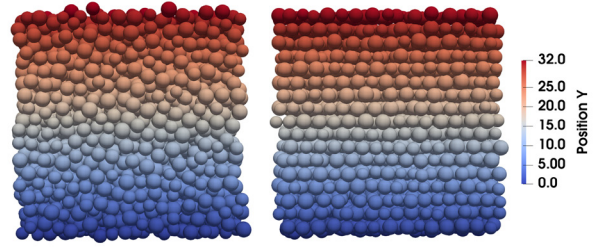


**Figure 3.** Visualisation of the structural layering effect with volume fraction  $\phi = 0.55$  at shear rate  $\dot{\gamma} = 1 \times 10^{-3}$ . Two different shear states are presented here: the initial transient state (left) and the end steady state (right). Colorbar indicates the particle positions in  $y$ -direction.

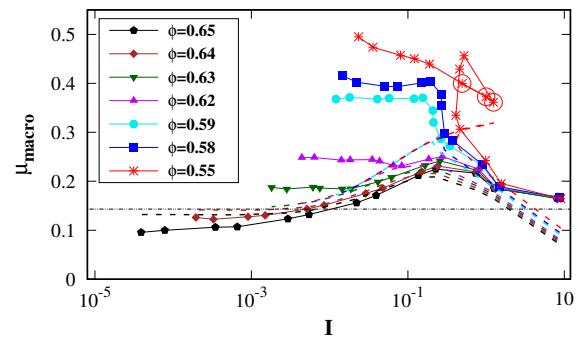


**Figure 4.** Bulk friction,  $\mu = \tau/p$ , plotted against the dimensionless shear rate,  $I$ , for different volume fractions, as given in the legend, from the same data as in Fig. 2. The dashed lines represent the rheology reported in Ref. [19].

shear rates and intermediate pressure. The lower densities for small enough  $p^*$  should be described by standard kinetic theory (data not shown), however, this is beyond the scope of this short paper.

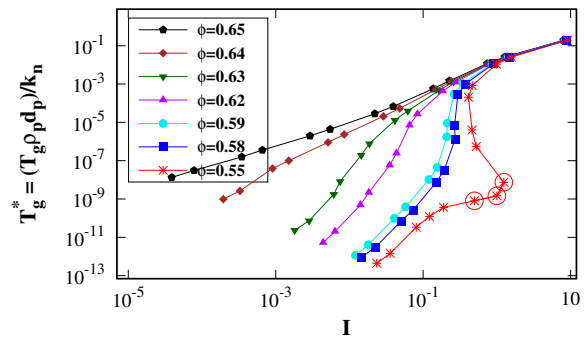


**Figure 5.** Dimensionless granular temperature,  $T_g^*$ , plotted against Inertial Number,  $I$ , for the same data as in Fig. 2.

Fig. 5 shows the dimensionless granular temperature  $T_g^*$  increasing with Inertial Number  $I$ , and softness,  $p^*$  (data not shown). The lower the density, the steeper

the increase for small volume fractions, from very sharp ( $\phi = 0.59, 0.58$ ) to a discontinuous kink (for  $\phi = 0.55$ ). Increasing shear rate or volume fraction (pressure) leads to more collisions among particles and thus “hotter” systems with higher granular temperature.

## 4 Conclusion

This study focused on the continuous and discontinuous shear thickening of friction- and cohesionless granular media, under constant volume shear. The constant stress rheology from a previous study [19] compares poorly with the constant volume cases (i) below jamming, and (ii) for strong compression – suggesting necessary improvements for the transitional regime in both the more dilute and the higher confining stress situations. Work in progress concerns even lower densities that agree well with SKT.

For frictionless packings, only CST is observed at lower volume fractions ( $\phi < 0.64 \approx \text{RCP}$ ) in the shear rate range investigated. Interestingly, a discontinuous “kink” appears in the flow curve of  $\phi = 0.55$  at shear rates around  $10^{-3}$ , caused by structural patterning (layering), which decreases shear resistance and pressure, while increasing  $I$ .

On the other hand, viscosity increases with density, from unjammed to jammed states, while the macroscopic friction shows an opposite trend, decreasing with  $\phi$ , and also at high confining stress and shear rate due to the increasing soft particles overlap.

In future, the micro-mechanical origin of the structural layering will be further investigated, e.g., interlayer particle migration, local velocity fluctuations, collision-driven instabilities possibly destabilizing the ordered state, as well as time dependent features during transitions. Further efforts will focus on unifying the standard kinetic theory (SKT) for low-density regimes with rheological models applicable at higher densities, under both volume- and stress-controlled shear configurations. The role of the missing ingredient – granular temperature – will also be further investigated.

## Acknowledgments

We would like to thank the EU for their financial support through the Marie Curie Initial Training Network: “T-MAPPP” (ITN607453).

## References

- [1] S. Luding, Y. Jiang, M. Liu, Un-jamming due to energetic instability: statics to dynamics, *Granular Matter* **23**, 80 (2021).
- [2] N. Kumar, S. Luding, Memory of jamming-multiscale models for soft and granular matter, *Granular matter* **18**, 1 (2016).
- [3] M. Van Hecke, Jamming of soft particles: Geometry, mechanics, scaling and isostaticity, *J. Phys. Condens. Matter* **22**, 33101 (2010).
- [4] G.D.R. MiDi, On dense granular flows, *European Physical Journal E: Soft Matter* **14**, 341 (2004).
- [5] I.R. Peters, S. Majumdar, H.M. Jaeger, Direct observation of dynamic shear jamming in dense suspensions, *Nature* **532**, 214 (2016).
- [6] R.L. Hoffman, Discontinuous and dilatant viscosity behavior in concentrated suspensions. I. Observation of a flow instability, *Transactions of the Society of Rheology* **16**, 155 (1972).
- [7] J.F. Morris, Shear thickening of concentrated suspensions: Recent developments and relation to other phenomena, *Annual Review of Fluid Mechanics* **52**, 121 (2020).
- [8] O. Sedes, A. Singh, J.F. Morris, Fluctuations at the onset of discontinuous shear thickening in a suspension, *Journal of Rheology* **64**, 309 (2020).
- [9] A. Singh, C. Ness, R. Seto, J.J. de Pablo, H.M. Jaeger, Shear thickening and jamming of dense suspensions: The “roll” of friction, *Physical Review Letters* **124**, 248005 (2020).
- [10] S.R. Waitukaitis, H.M. Jaeger, Impact-activated solidification of dense suspensions via dynamic jamming fronts, *Nature* **487**, 205 (2012).
- [11] X. Cheng, J.H. McCoy, J.N. Israelachvili, I. Cohen, Imaging the microscopic structure of shear thinning and thickening colloidal suspensions, *Science (New York, N.Y.)* **333**, 1276 (2011).
- [12] J.R. Royer, D.L. Blair, S.D. Hudson, Rheological signature of frictional interactions in shear thickening suspensions, *Physical review letters* **116**, 188301 (2016).
- [13] A. Singh, S. Pednekar, J. Chun, M.M. Denn, J.F. Morris, From yielding to shear jamming in a cohesive frictional suspension, *Physical review letters* **122**, 098004 (2019).
- [14] R. Seto, A. Singh, B. Chakraborty, M.M. Denn, J.F. Morris, Shear jamming and fragility in dense suspensions, *Granular Matter* **21**, 82 (2019).
- [15] O. Pouliquen, Powders and cohesive granular media: a rheological perspective, *Rheologica Acta* pp. 1–13 (2025).
- [16] A. Singh, V. Magnanimo, K. Saitoh, S. Luding, The role of gravity or pressure and contact stiffness in granular rheology, *New Journal of Physics* **17**, 043028 (2015).
- [17] S. Luding, Cohesive, frictional powders: Contact models for tension, *Granular Matter* **10**, 235 (2008).
- [18] S. Luding, Collisions Contacts between Two Particles, in *Physics of Dry Granular Media - NATO ASI Series E350*, edited by H.J. Herrmann, J.P. Hovi, S. Luding (Kluwer Academic Publishers, Dordrecht, 1998), p. 285
- [19] H. Shi, S. Roy, T. Weinhart, V. Magnanimo, S. Luding, Steady state rheology of homogeneous and inhomogeneous cohesive granular materials, *Granul. Matter.* **22**, 14 (2020).
- [20] S. Roy, S. Luding, T. Weinhart, A general(ized) local rheology for wet granular materials, *New Journal of Physics* **19**, 043014 (2017).